

Synthesis, characterization of CdS/rectorite nanocomposites and its photocatalytic activity

Jiangrong Xiao · Tianyou Peng · Dingning Ke ·
Ling Zan · Zhenghe Peng

Received: 15 August 2006 / Accepted: 2 February 2007 / Published online: 17 February 2007
© Springer-Verlag 2007

Abstract CdS/rectorite nanocomposite was synthesized via a cation-exchange reaction followed by a sulfurization process. The obtained samples were characterized by using X-ray diffraction (XRD), fourier transform infrared spectra (FTIR), transmission electron microscope (TEM), UV-Vis diffuse reflectance spectra (DRS), and thermal analysis. The measured results indicate that CdS species in the composites exist in the form of pillars and nanoparticles, the crystallized CdS particles are in the hexagonal symmetry. The photocatalytic activities of the pillared nanocomposite were enhanced significantly comparing with the bare rectorite and the pure CdS. Moreover, the photostabilities of the obtained nanocomposites are also better than that of the pure CdS due to the hosts retard the photocorrosion of the CdS.

Keywords CdS · Pillared rectorite · Nanocomposites · Photocatalytic activity

Introduction

Rectorite is an interstratified layered silicate mineral consisting of montmorillonite-like layers and mica-like

layers in a regular stacking (1:1 ratio) with about 2.46 nm interlayer spacing (Grim 1968). The cations of Na^+ , K^+ , Mg^{2+} and Ca^{2+} lie in the intergallery spaces of 2:1 montmorillonite-like and 2:1 mica-like layers, but only the hydrated cations distributed in the montmorillonite-like layers are exchangeable (Brindley 1956). Due to its structure similar to the montmorillonite, rectorite has some excellent properties like montmorillonite mineral, such as high heat resistance, good colloidal property in water, good plastic index and processing properties, it is potential in many industrial applications, especially in the absorber, high-grade lubricant, and the catalyst in the oil gas decompositions etc. (HuBei Province Geology and Mineral Office 1989). At the same time, mica-like layers as a support make the rectorite more stable than montmorillonite, as well as the montmorillonite-like layers in the rectorite have exchangeable ion species (Brindley 1956). Therefore, rectorite may be a more suitable host for the pillared structures compared with the montmorillonite clay.

In the past decades, rectorites with various pillared structures have been prepared and characterized (Occelli et al. 2000a, b; Thomas and Occelli 2000; Occelli and Gould 2001; Occelli et al. 1993; Pichowicz and Mokaya 2004; Ohtsuka 1997), which are extensively applied as absorber and catalyst in many industrial fields due to its cracking activity, gasoline selectivity, adsorption property and metal resistance (Occelli et al. 1993, 2000; Zhang et al. 2004, 2005). For example, alumina-pillared rectorites have been synthesized from the reaction between the rectorite and an aluminum chlorhydroxide solution containing the dodecameric $[\text{Al}_{13}\text{O}_4(\text{OH})_{24}(\text{H}_2\text{O})_{12}]^{7+}$ ion. And an atomic force microscope (AFM) has been used to

J. Xiao · T. Peng (✉) · D. Ke · L. Zan · Z. Peng
Department of Chemistry, Centre of Nanoscience
and Nanotechnology Research, Wuhan University,
Wuhan 430072, China
e-mail: typeng@whu.edu.cn

T. Peng
State Key Laboratory of Coordination Chemistry,
Nanjing University, Nanjing, China

investigate the surfaces of the pillared rectorite products after various processes (e.g. annealing and hydrothermal treatment, as well as the catalyst after gas oil cracking process). The results showed that the dodecameric $[\text{Al}_{13}\text{O}_4(\text{OH})_{24}(\text{H}_2\text{O})_{12}]^{7+}$ ion were located in the montmorillonite-like interlayer of rectorite (Occelli and Gould 2001). And 0.13 mmol dodecameric ions per gram clay were required for the structural stability (Thomas and Occelli 2000). Simultaneously, alumina-pillared rectorite as catalyst for the gas oil cracking under microactivity testing (MAT) conditions (100% steam at 760°C and 1 atm) has also been reported. After steaming for 5 h under the MAT conditions, the pillared rectorite can crack gas oil with 85.2% conversion and 59.5% gasoline generation (Occelli 1991).

Recently, the composites of cadmium sulfide (CdS) with various inorganic substances have received much attention. CdS itself is a semiconducting material, besides its interesting optical properties (Schwerzel et al. 1998; Sapra et al. 2001), the semiconductor is also interesting for the special photocatalytic activity and it is active under visible light for hydrogen production from photosplitting water (Minoura and Tsuiki 1978). CdS is not stable in aqueous solutions under irradiation due to electrochemical corrosion, but it has been reported that the supported CdS has a performance and stability superior to that of the unsupported one, because the active ingredient is dispersed on the supports, and the supports provide heterojunctions for the photogenerated electrons and holes that restrict the charge recombination and S^{2-} oxidation (Sato et al. 1996a, b; Shangguan and Yoshida 2001). For example, CdS has been intercalated into the interlayers of semiconducting layered compounds to form CdS/ $\text{H}_2\text{Ti}_4\text{O}_9$, CdS/ $\text{K}_2\text{Ti}_4\text{O}_9$, and CdS/ $\text{H}_4\text{Nb}_6\text{O}_{17}$ compositions. (Sato et al. 1996a, b; Shangguan and Yoshida 2001) Shangguan and co-workers have reported that the photoactivities of CdS/ $\text{K}_2\text{Ti}_4\text{O}_9$, CdS/ $\text{K}_2\text{Ti}_{3.9}\text{Nb}_{0.1}\text{O}_9$ were superior to those of the pure CdS and the physical mixture of CdS and metal oxides (Shangguan and Yoshida 2001). Moreover, CdS has also been incorporated with mesoporous materials including SBA-15 silica (Wang et al. 2002), MCM-41 silica (Zhang et al. 2001), and porous alumina (Arora et al. 1998, 1999) to produce size-confined CdS nanoparticles within those matrixes. Hirai and co-workers have also investigated the size-selective incorporation of CdS nanoparticles into mesoporous silicate, the resulting composites showed a good activity for H_2 generation from photosplitting water (Hirai et al. 1999). Furthermore, CdS-pillared montmorillonite has also been researched extensively (Dekany et al. 1999a, b; Han et al. 2005; Fujishiro et al.

1999). Recently, a hydrothermal synthesis method for the CdS/montmorillonite composites, in which the CdS exists in the pillared forms and nanoparticles, has also been reported (Han et al. 2005).

Rectorite is a kind of rare mineral in the world, but there are rich resources in the two county of Zhongxiang and Nanzhang, Hubei Province, China. Although the pillared rectorites as catalysts have been studied extensively (Occelli et al. 2000a, b; Occelli 1991), those researches mainly concentrated on the oil gas decompositions. Up till now, rectorite has seldom been applied in the photodegradation of organic contaminations as photocatalyst. Considering that the rectorite is a more suitable host for the pillared structures than montmorillonite as described above (Yamanaka et al. 1990; Malla et al. 1989), and CdS is a kind of semiconductor with photoactivity which can absorb UV and visible light. The CdS/rectorite pillared composites may have some promising applications in the photocatalysts for the degradation of contaminations and hydrogen production of photosplitting water. To the best of our knowledge, however, there is still no literature reported on the synthesis and its photocatalytic performances of the CdS-pillared rectorite. Herein, CdS/rectorite pillared nanocomposites were synthesized via an ion-exchange reaction followed by a sulfurization process. The microstructures were characterized by using XRD, FTIR, DRS, TEM and thermal analysis. The experimental results indicated that the photoactivities and photostabilities of the obtained nanocomposites were improved to some extent compared to that of the bare rectorite and the pure CdS.

Experimental section

Materials

Rectorite was produced from Zhongxiang County, and supplied by Hubei Celebrities Rectorite Technology Co. Ltd, China. The composition of rectorite are listed in Table 1 (GBW(E)070063), as can be seen, impurities, such as, TiO_2 and Fe_2O_3 , coexisted in the rectorite clay. The cation exchange capacity (CEC) is 44.9 meq/100 g, the bulk resistivity is about $10^8 \Omega \text{ cm}$, and the average particle size is 0.82 μm . The d -spacing (d_{001}) is 2.46 nm, which is contribution from the mica-like layer (d -spacing is ca. 0.96 nm) and the montmorillonite-like layer (d -spacing is ca. 1.50 nm). Cadmium acetate ($\text{CdAc}_2 \cdot 2\text{H}_2\text{O}$, AR, Sinopharm Chemical Agent Co., China), FeS (CP, Shanghai Chemical Agent Factory, China), H_2SO_4 (AR, Shanghai Chemical Agent Factory,

Table 1 The compositions of the rectorite (GBW(E)070063)

Component	SiO ₂	Al ₂ O ₃	Fe ₂ O ₃	CaO	MgO	TiO ₂	K ₂ O	Na ₂ O	MnO	P ₂ O ₅	F
Mass (%)	44.31	35.60	1.50	4.05	0.35	2.46	1.12	1.24	0.01	0.41	0.08

China) and Rhodamine B (AR, Shanghai Agents Company, China) were used as received. All the other reagents used without further purification. Throughout of the present study the water used was distilled water.

Preparation of CdS/rectorite nanocomposite

The preparation of CdS/rectorite nanocomposite includes an ion-exchange reaction and followed by a sulfurization process. In a typical process, 4.0 g of rectorite was dispersed into 100 ml of distilled water with stirring vigorously to obtain 4.0 wt.% suspension. And subsequently, 0.2 mol/l CdAc₂ solution with different volume was added stepwise into above suspension under strongly stirring. The molar ratio of Cd²⁺/rectorite was changed from 0 to 4.0 mmol/g. The mixture was stirred continually for another 72 h at room temperature. And then the precipitate was centrifuged, washed with distilled water to remove the excess CdAc₂ until the supernatant was free of Cd²⁺ ions indicated by a 0.2 mol/l Na₂S aqueous solution. The resulting precipitate was dried at 60°C for 6 h to obtain the ion-exchanged sample. The dried ion-exchanged sample was re-dispersed in water for 4 h under stirring, and then H₂S gas generated from FeS and 3.0 mol/l H₂SO₄ in Kipp apparatus, was introduced into the suspension for 2 h. The CdS/rectorite nanocomposite was recovered by centrifugation, washed with water, and then dried at 80°C for another 4 h. For the convenience of description, the nominal amount of CdS was used to denote the corresponding product. For example, 4.0 mmol/g CdS/rectorite is obtained from the 80 ml of 0.2 mol/l CdAc₂ and 100 ml of 4.0 wt.% rectorite suspensions. For comparison, pure CdS was also prepared by introducing H₂S gas into 0.2 mol/l CdAc₂ solution.

Characterization of products

The XRD patterns of the prepared products were recorded by using a XRD-6000 powder diffractometer (Shimadzu, Japan) with Cu-K α as a radiation. FTIR spectra on pellets of the samples with KBr were recorded on a FTIR-8201PC spectrometer (Nicolet, America). Transmission electron microscope images and microanalysis were obtained on a LaB6 JEM-2010 (HT)-FEF electron microscope (HRTEM, Japan Electronics, Japan). UV-Vis diffuse reflectance spectra (DRS)

were performed with a Cary 5000 UV-Vis-NIR spectrophotometer equipped with an integrating sphere (Varian, America). Thermogravimetry (TG) and differential thermal analysis (DTA) curves were recorded on a STA 449 thermal analyzer (Netzsch, Germany). Cadmium ions remaining in the collected supernatant during the separation and wash processes were determined by inductively coupled plasma atomic emission spectrometry (ICP-AES, Beijing Broadcast Instrument Factory, Beijing, China). This, in turn, permitted the assessment of the inserted amount of Cd²⁺ in the rectorite.

Photocatalytic activity tests

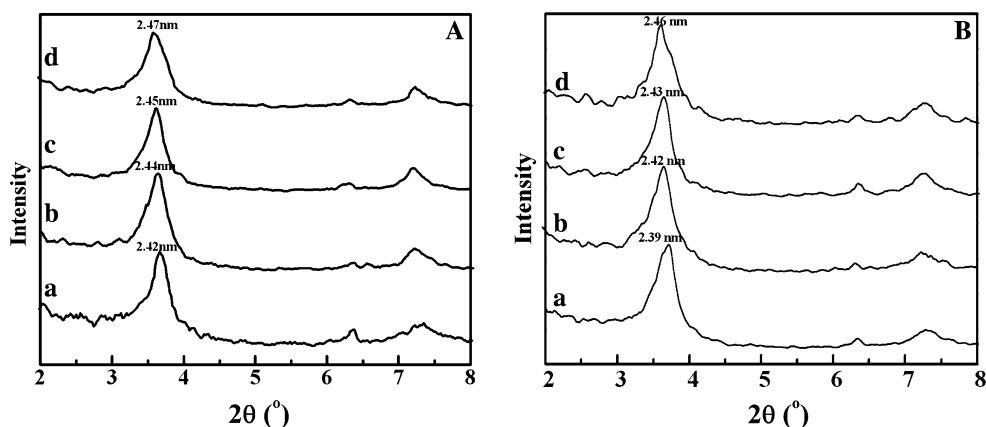
All photodegradation of Rhodamine B (RB) processes were conducted at ambient pressure and room temperature. The light source was a 250 W Hg lamp, a surrounding water jacket (Pyrex) to cool the lamp. In a typical process, 0.0300 g of 4.0 mmol/g CdS/rectorite nanocomposite was added into 50 ml of 5.0 mg/l RB aqueous solution (pH 6.0). Before irradiation, the suspension was magnetically stirred for 45 min in the dark (to adsorption equilibrium of RB on the surfaces of photocatalyst). After irradiation, the photocatalyst was removed by centrifugation, and the supernatant was examined using a Shimadzu UV-240 spectrophotometer. For comparison, the bare rectorite, the pure CdS and their physical mixture were also been conducted under an identical experimental condition. For evaluating the photostability of the products, the photodegradation experiments of the same photocatalyst were repeated for several times under an identical experimental condition too.

Results and discussion

X-ray diffraction analysis

The low-angle XRD patterns of the bare rectorite, 1.0, 2.0 and 4.0 mmol/g CdS/rectorite nanocomposite dried at 80°C are shown in Fig. 1a. As can be seen, the d₀₀₁ diffraction peaks at 2 θ = 3.65° for the bare rectorite are corresponding to the d-spacing of 2.42 nm, which is similar with the reference value as described above. The d-spacings are found to shift from 2.42 nm

Fig. 1 Low-angle X-ray diffraction (XRD) patterns of the products dried at 80°C (**a**) and 170°C (**b**). **a** Bare rectorite, **b** 1.0 mmol/g, **c** 2.0 mmol/g and, **d** 4.0 mmol/g CdS/rectorite



($2\theta = 3.65^\circ$) to 2.47 nm ($2\theta = 3.58^\circ$) upon increasing the nominal amount from 0 to 4.0 mmol CdS per gram rectorite, implying that the CdS had inserted into the intergallery spaces of montmorillonite-like layers in the rectorite (Occelli and Gould 2001; Han et al. 2005). The progressive decrease of the intensity and concomitant broadening of the diffraction peaks upon CdS intercalation into intergallery spaces in the rectorite indicate an uneven stretching of the lamellas upon the formation of CdS pillars and a decrease of their uniformity.

The above interlayer expansion of the CdS/rectorite may be ascribed to the water adsorbed in the interlayer rather than due to the CdS pillars, because the 80°C drying process cannot remove the water completely. As observation from the thermal analysis result in Fig. 4, absolute majority of water can be removed in the range of 25–170°C. Therefore, the 80°C dried products were treated at 170°C for 3 h to remove the water adsorbed in the samples. The low-angle XRD patterns of such heated samples in Fig. 1b reveal that the d_{001} diffraction peaks occur at a progressively lower angle as the nominal amount increases from 0 to 4.0 mmol CdS per gram rectorite (e.g. from $2\theta = 3.70^\circ$ to 3.59° , the corresponding d-spacings from 2.39 to 2.46 nm). The change of the d_{001} peak position reveals that the d-spacing of the rectorite remains expanded after the heat treatment for all the 80°C dried CdS/rectorite. On the other hand, the corresponding heated products have the d_{001} peaks systematically shifted to a higher angle, indicating a systematic contraction of the intergallery distance. The contraction may be ascribed to the removal of the water adsorbed in the interlayers of the products. For instance, the d-spacings are found to shift from 2.42 nm ($2\theta = 3.65^\circ$) to 2.39 nm ($2\theta = 3.70^\circ$) upon heating at 170°C for the bare samples, which is similar with the previous literature (2.32 nm) (Kooli et al. 1997); whereas, the d-spacings are just found to give a very slightly contraction for the

nominal 4.0 mmol/g CdS/rectorite, implying that there is fewer adsorbed water in the 4.0 mmol/g nanocomposite than the bare one, which is consistent with the results of the following thermal analysis (Fig. 4). Those results indicate that there are solid species, putatively the CdS pillars, which are tightly bound in the intergallery spaces of the rectorite, and this is reasonable result of the cation-exchange and sulfurization processes. The shift of d_{001} diffraction peak reflects the thickness of the CdS pillars. A higher amount CdAc₂ leads to a higher equilibrium Cd²⁺ concentration in the interlayers of the rectorite, consequently, produces CdS pillars with larger sizes by the subsequent sulfurization process, expanding the d-spacing. The average sizes of the pillars in the different products are very small. A similar result (ca. 0.18 nm shifts of the d-spacings) has also been previously reported for the CdS/montmorillonite composite synthesized through a hydrothermal process (Han et al. 2005).

The high-angle XRD patterns of the bare rectorite, 1.0 and 4.0 mmol/g CdS/rectorite nanocomposite are shown in Fig. 2. As evidenced from Fig. 2b, c, the diffraction traces at $2\theta = 24.8^\circ$, 26.5° , 28.3° , 43.7° , and 51.8° (denoted by asterisk in Fig. 2) can be ascribed to the hexagonal CdS crystal phase (JCPDS no. 41-1049, P6₃mc; $a = 0.41409$ nm, $c = 0.67198$ nm) and, those diffraction peaks become more apparent and sharper as the nominal CdS amount increases. On one hand, the increasingly sharper diffraction peaks of the CdS suggest that the CdS crystallites with a larger particle size are produced in the intergallery space of rectorite when the nominal amount of CdS increased. This increase is logical simply because more Cd²⁺ feed will be more favorable to the production and crystal growth of the CdS during the sulfurization reaction. On the other hand, except for CdS species existing in the forms of pillars inside rectorite, some more CdS nanoparticles may also formed in the outer layer of rectorite upon increasing the nominal amount of CdS. On the

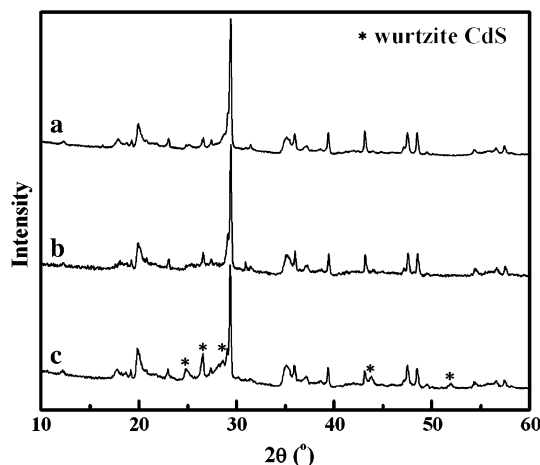


Fig. 2 High-angle X-ray diffraction (XRD) patterns of the products. **a** Bare rectorite, **b** 1.0 mmol/g and, **c** 4.0 mmol/g CdS/rectorite

contrary, less Cd^{2+} feed is unfavorable to the crystal growth or even cannot afford CdS nanoparticles. However, due to low driving force and the thermodynamics factors in the present conditions, the pillared particle sizes are still very small (Han et al. 2005; Kooli et al. 1997).

FTIR spectra

Figure 3 show the FTIR spectra of the bare rectorite, 1.0 and 4.0 mmol/g CdS/rectorite nanocomposite. There are five pairs of peaks at ca. 478/542, 714/745, 905/930, 1019/1048 and 1082/1119 cm^{-1} in all of the samples, which are the characteristic peaks contributed from the rectorite (Kooli et al. 1997; Xie et al. 2004). Peaks located at the intermediate frequency regions are changeless and the intensities of these peaks are decreased slightly as the nominal amount of CdS increase, implying that the silicate layer structures of the rectorite are remained during the prepared process. And the intensity of the peak at 480 cm^{-1} is stronger than that at 416 cm^{-1} in the FTIR spectra of the all products, which suggests that the products are remained the 1:1 interstratified regular stacking structure of double octahedron montmorillonite-like crystallite at 2:1 ratio and mica-like crystallite at 2:1 ratio, which is also consistent with the observation from the XRD.

It is believed that the broad peaks at ca. 3,636, 3,400 and 1,634 cm^{-1} are attributed to the surface-adsorbed water and the hydroxyl groups (Xie et al. 2004). The intensities of the broad peaks at around 3,400 cm^{-1} , which is ascribed to the surface-adsorbed water, decrease as the nominal amount of CdS per rectorite increase, suggesting that the CdS-pillars partly deplete

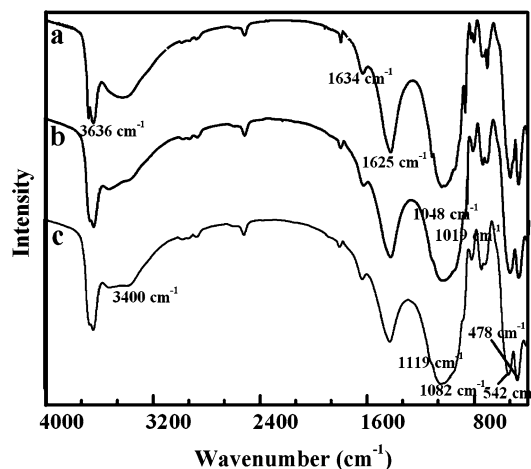


Fig. 3 FT-IR spectra of the products. **a** Bare rectorite, **b** 1.0 mmol/g and, **c** 4.0 mmol/g CdS/rectorite

the adsorbed water in the intergallery regions of rectorite, which will be further discussed in the following section. The intensities of peaks (e.g., ca. 874 and 916 cm^{-1}) arising from the hydroxide (OH) deformations linked to Al and/or Mg ions for the CdS/rectorite nanocomposites are lower than the bare rectorite. Breakup of the rectorite particles may affect the position or environment (e.g., nearest neighbor atoms) of these metal ions, thus reducing the intensity of the structural OH groups linked to them. Moreover, it is also expected to result in an increase in terminal OH groups. This can be observed by the relative increase in the intensity of the OH peak at ca. 3,636 cm^{-1} in Fig. 3 for the CdS/rectorite nanocomposites. All of above observations indicate that the basic stacking structure of the rectorite remained unchanged and the changes in constitute mainly occurred in the intergallery spaces of the rectorite.

Thermal analysis

Figure 4 shows the thermogravimetry analysis (TGA) plots of the bare rectorite and 4.0 mmol/g CdS/rectorite pillared nanocomposite under N_2 atmosphere. As can be seen from Fig. 4b, there are remarkable three step weight loss courses for the CdS/rectorite. The first weight loss with 3.57% in the range of 25–170°C is mainly attributed to the removal of the adsorbed water, which is followed by a trace weight loss between 170 and 400°C. The second step weight loss with 4.44% in the range of 400–670°C is probably ascribed to the dehydroxylation of the OH groups. Finally, an additional weight loss with 8.91% in the range of 670–1,000°C can be assigned to the dehydroxylation (O–H bands) of structural silicate layers of the clay (Lu et al.

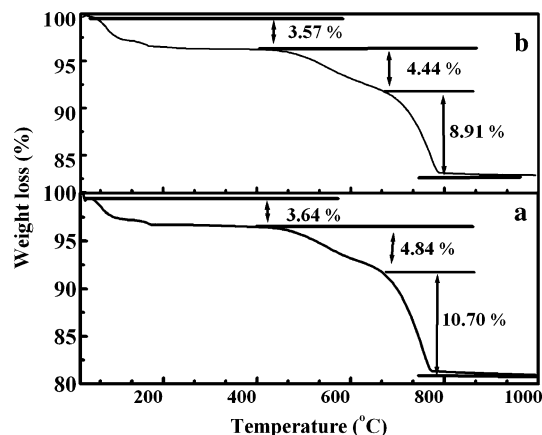


Fig. 4 Thermogravimetry analysis (TGA) curves of the products. **a** Bare rectorite and, **b** 4.0 mmol/g CdS/rectorite

2001) When the samples are treated from 25 to 1,000°C, the total weight loss of the 4.0 mmol/l CdS/rectorite is 16.92%. For the bare rectorite, there are also remarkable three step weight loss courses with 3.64, 4.84, and 10.70%, respectively. The total weight loss, however, is 19.18%. It is clear that the lower weight loss for the 4.0 mmol/g CdS/rectorite is contributed from the CdS, which partly depleted the absorbed water and hydroxyl group in the intergallery regions of the rectorite during the present experimental procedures; this is consistent with the above results of the low-angle XRD and FTIR. As can be seen from the DTA curves (not shown) the dehydroxylation (O–H bands) peak of silicate layers in the bare rectorite occur at 763.7°C with 10.70% weight loss, whereas the corresponding dehydroxylation peak for the 4.0 mmol/g CdS/rectorite occur in 778.3°C with 9.56% weight loss. It seems that the thermal stability of the nanocomposites has been enhanced slightly by the CdS intercalating into rectorite host.

Some clues that the CdS inserted mainly into the rectorites accompanied with small amount CdS nanoparticles absorbed in the outer space of the rectorites can be drawn from the difference of total weight loss

between CdS/rectorite and the bare one. To further clarify this, the amount of Cd²⁺ was determined by ICP-AES, the supernatant during the separation and wash processes were collected and Cd²⁺ ion remaining in the collected solution was determined. This, in turn, permitted the assessment of the amount of CdS in the rectorite. The experimental results show that 0.0806 g Cd²⁺ per gram rectorite had been lied in the nominal amount of 4.0 mmol/g CdS/rectorite. Namely, the amount of CdS in the composite is about 9.39 wt.%. Considering that the precipitate was washed with distilled water to remove the excess CdAc₂ until the supernatant was free of Cd²⁺ ions indicated by a 0.2 mol/l Na₂S aqueous solution after the ion-exchange process with 0.2 mol/l CdAc₂ solution, therefore, we think that the forms of CdS is mainly pillars inside the interlayer accompanied with very small amount CdS nanoparticles absorbed the outer space of rectorites.

Microstructure analysis

Figures 5, 6, 7 show the TEM images, microanalysis and EDXS results of the 4.0 mmol/g CdS/rectorite. For the purpose of comparison, the unwashed sample was also synthesized, namely, the precipitate after the Cd²⁺ ion-exchanges stage was not washed by water, and then directly dried and followed by the sulfurization process. As can be seen from Fig. 5a, the unwashed samples show a large amount of nanoparticles absorbed on the surface, the particle sizes are in the range of 4–16 nm with average particle size of 8.5 nm; whereas, a few of particles are observed on the surface of the washed product (Fig. 5b). Namely, the washing procedure can effectively remove the surface-absorbed Cd²⁺, therefore, there is seldom CdS particle formed on the surface of the rectorite.

Figure 6a shows a HRTEM image of the 4.0 mmol/g CdS/rectorite containing some darker patches, the putative CdS nanoparticles, with a relatively monodispersed particles (average grain size of ca. 4.2 nm), which is much smaller than those of the nanoparticles

Fig. 5 TEM micrographs of the nominal amount 4.0 mmol/g CdS/rectorite. **a** Unwashed and, **b** washed product

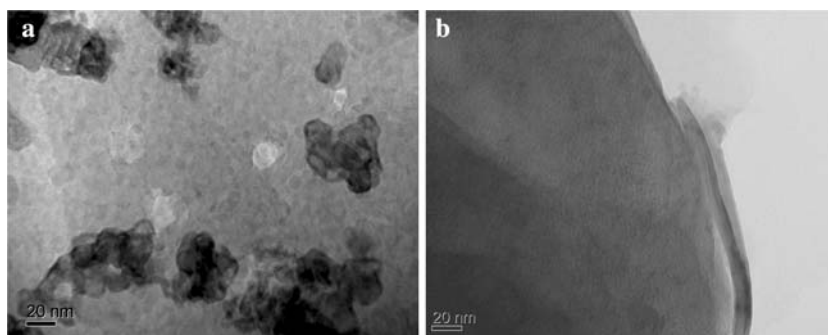


Fig. 6 HRTEM images of the 4.0 mmol/g CdS/rectorite. **a** A general region containing CdS nanoparticles and the SAED pattern, **b** a CdS nanoparticles grain in the host, **c** a general region for the elemental analysis and, **d** EDXS result of a dark region in the selected area

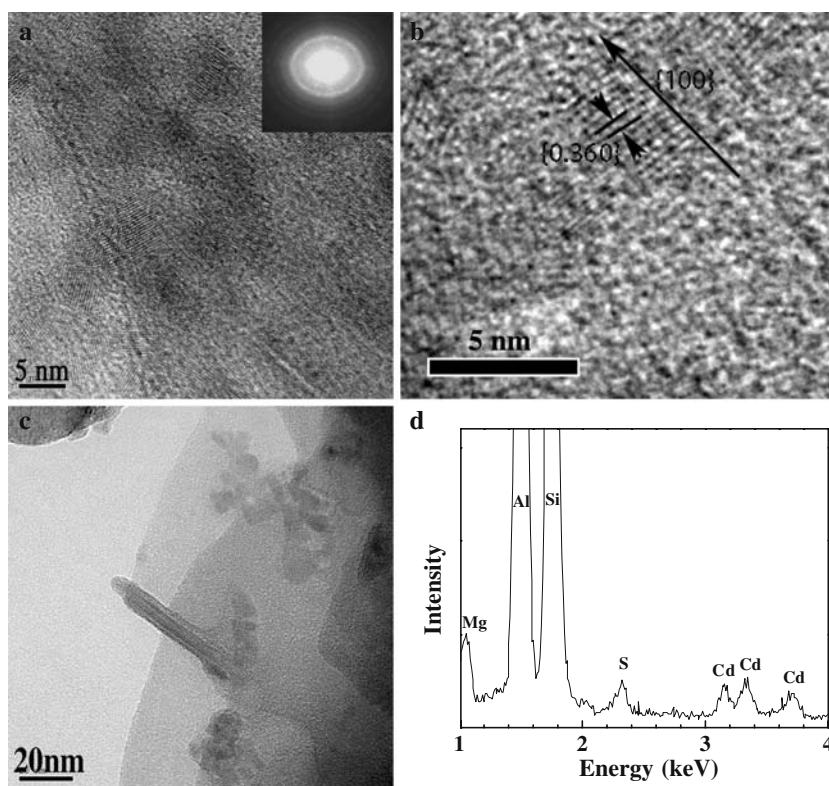
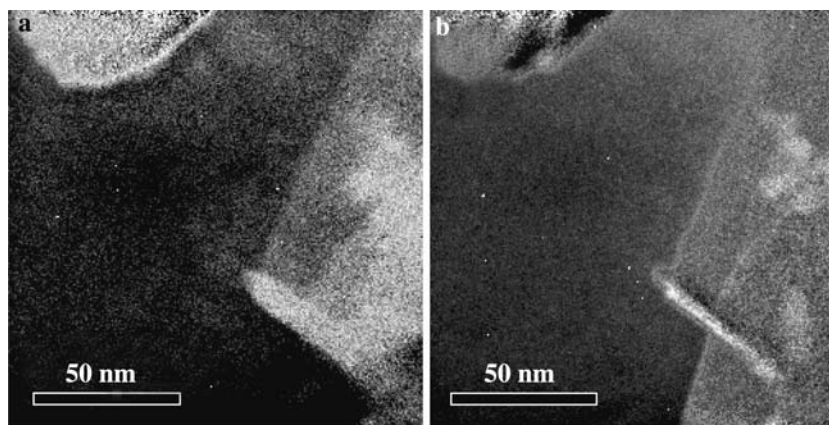


Fig. 7 Elemental mapping of the HRTEM image in Fig. 6 for the 4.0 mmol/g CdS/rectorite. **a** Cd, and, **b** S



observed on the surface of the unwashed product. Moreover, it is not so distinguishable, implying that the nanoparticles mostly located between the intergallery regions in the rectorite. Those observations may be ascribed to that the crystallite growth of the inserted CdS particles are confined by the host matrix, and that the relative lower driving force of intercalation in the present experimental conditions. Generally, the layer distance should be expanded by those CdS particle about 4 nm in diameter incorporated in the interlayer. However, there is no significant peak shift as observation in LAXRD (Fig. 1). The possible explanation for this contradiction may be that the CdS particles may be flat in shape due to the restriction of the host matrix,

and about 4 nm in diameter is the projective region of CdS. Moreover, rectorite is an interstratified layered silicate mineral consisting of montmorillonite-like layers and mica-like layers in a regular stacking (1:1 ratio) with about 2.46 nm interlayer spacing, which is contribution from the mica-like layer (d-spacing is ca. 0.96 nm) and the montmorillonite-like layer (d-spacing is ca. 1.50 nm) (Grim 1968). Considering that the CdS particles mainly lie in the intergallery spaces of 2:1 montmorillonite-like layers, and the relative small proportion of CdS amount and the montmorillonite layers in the nanocomposite, it is reasonable that there is no significant peak shift in LAXRD after CdS incorporated into rectorite (Fig. 1).

The selected area electron diffraction (SAED) pattern in Fig. 6a shows that the surrounding of the crystalline CdS phase is polycrystalline and amorphous clay phase. The diffraction dots are also distinguishable, which is consistent with the wurtzite CdS crystal (JCPDS no.41–1049) of hexagonal symmetry. Figure 6b provides a HRTEM image showing a CdS grain in the composite. The CdS crystallite shows regular projection lines of the [100] crystal plane, and the distance between the crystal planes is 0.3600 nm, which is in agreement with the reference data of CdS (0.3586 nm). The surrounding of the CdS crystallite with a distinctive contrast with matrix is an amorphous phase in the image. The rectorite was crystalline according to above XRD, but it appeared to be extremely sensitive to the high voltage of TEM, and the crystal phase was vitrified to an amorphous immediately by the electron beam. It is desirable if the products are applied for hydrogen production from photosplitting water, because the hexagonal CdS has a better photoactivity than the cubic CdS (Arora et al. 1998, 1999).

Figure 6d shows the result of energy dispersive spectrometry (EDXS) from the tenebrous region. It is demonstrated that besides Cd and S from the CdS, Mg, Al and Si from the rectorite are also presented, as would be expected (Hong et al. 2005). Quantitative analysis result reveals that the contents of Cd and S are 48.99 and 51.01%, respectively. Although it is fairly close to 1:1 corresponding with the CdS formula, the contents of S in general area are always excessive over those of the Cd, which can be ascribed to the samples containing trace amount of S in the rectorite according to the supplier. The TEM image providing an overview of a general region of the sample is shown in Fig. 6c. The mappings for the distribution of Cd and S in such region of Fig. 6c are presented in Fig. 7a, b. The discrete signals from Cd and S in the rectorite host structure are found. And the bright dots show clear signals and mainly distribute in the main body of the rectorite host but not just in the surface, which suggests that the CdS particles mostly exist in the interlamellar of the rectorite in the 4.0 mmol/g CdS/rectorite. The presence of the two elements in the main body of the clay supports the conclusion that the expanded d-spacings arise from the CdS pillars in the intergallery space because the nanometer electron probe has stimulated discrete signals from Cd and S; the signals generated suggest these species are now intrinsic to the rectorite host structure. The faint dots denote weak signals, which are reasonable for the very low content of CdS pillars in the intergallery spaces of the composites. The CdS pillars intercalate into the intergallery spaces of the

rectorite host, so the basal d-spacing expands from 2.42 to 2.47 nm as observation from Fig. 1a.

Based on above XRD, microscopy and microanalysis, it is unambiguous that the darker patches in the product are CdS crystallites produced inside of the intergallery region of the rectorite, which are responsible for the diffraction peaks of the CdS in Fig. 2b, c. The obtained CdS nanoparticles in the composites make the present work distinctive from previous work that had not obtained CdS nanoparticles in a similar synthesis method. For instance, no CdS crystallite was observed in the CdS/laponite composites, even where the nominal CdS content reached 0.5 mmol/g clay (Stramel et al. 1986).

UV-Vis diffuse reflectance spectra (DRS)

The UV-Visible diffuse reflectance absorbance spectra (DRS) for the bare rectorite, 1.0, 4.0 mmol/g CdS/rectorite and its physical mixture are shown in Fig. 8. As can be seen, the bare rectorite showed visible light absorption ability. It is rational that the sample contained some impurity such as ferric oxide and titania as indication in Table 1. The CdS/rectorite composites induce only limited red shifts of the light absorption compared with the bare one, but the absorbance of the product significantly enhance in the observation range of 200–800 nm, and the red shifts in light absorption and increases in absorbance are found to increase as the nominal amount of CdS in the rectorite was enhanced, implying that the larger size CdS particles are generated in the intergallery spaces of the rectorite host. The red shift and increase trends of the absorbance in the CdS/rectorite are comparable to the observed result of the CdS/montmorillonite (Han et al. 2005; Kooli et al. 1997) and CdS/laponite clay (Stramel et al. 1986), where a red shift exhibited on the absorption onset when the exchanged concentration of Cd was increased.

Although the amount and the particle size of CdS in the 1.0 mmol/g products is much smaller than that of CdS in the physical mixture according to the nominal amount 4.0 mmol/g CdS/rectorite, the absorbance for the 1.0 mmol/g CdS/rectorite is higher in the range of 200–500 nm, which may be beneficial for the more effective light absorption and electron transfer in the CdS/rectorite composites due to the smaller particle size in the rectorite layers. Furthermore, the nanocomposites show that the absorption onset shifts to a lower wavelength as the CdS amount decreases. The shifting trend is consistent with the XRD and TEM results and suggests that smaller CdS nanoparticles are yielded when the amount Cd²⁺ decrease. On the other hand,

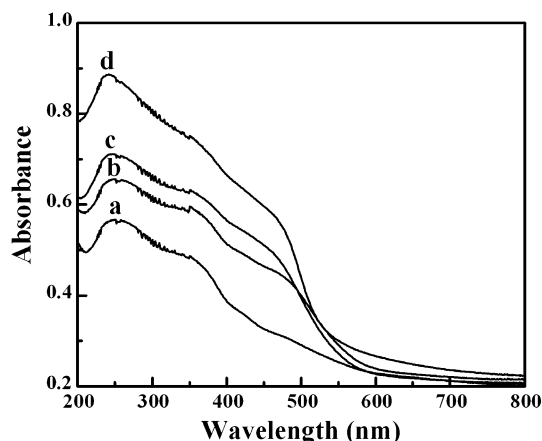


Fig. 8 Diffuse reflectance absorbance spectra (DRS) of the products. **a** Bare rectorite, **b** Physical mixture of CdS and rectorite according to nominal amount of 4.0 mmol/g CdS/rectorite, **c** 1.0 mmol/g and, **d** 4.0 mmol/g CdS/rectorite

the band gap energy of CdS intercalated composites is larger than that of the physical mixture of CdS and rectorite as shown in Fig. 8b–d. This difference can be attributed to the smaller particle sizes of CdS pillars in the pillared rectorite compared with the pure CdS. Namely, the incorporation of CdS nanoparticles into the intergallery spaces of the rectorite could suppress the particle growth. This, in turn, resulted in the quantum size effect, and consequently, the band gap energy enlarging (Katsikas et al. 1990).

Photocatalytic activity tests

By applying the photodegradation of Rhodamine B (RB) as a probe reaction, the photoactivity of the product as photocatalyst was also investigated by dispersing 30 mg of the 4.0 mmol/g CdS/rectorite into 50 ml of RB solution. The relations between the photodegradation efficiency (denoted as c_t/c_0) of RB and the time under a UV-Vis light irradiation are summarized in Fig. 9. For comparison, it also gives the photocatalytic experiment results of the bare rectorite, the physical mixture containing similar components and the pure CdS (11.0 mg) according to 30 mg 4.0 mmol/g CdS/rectorite, respectively. For the 4.0 mmol/g CdS/rectorite, photodegradation efficiency increases to 94.6% after 2 h irradiation; whereas, it just reaches 55.6, 76.0 and 63.5% for the bare rectorite, the pure CdS (11.0 mg) and the physical mixture, respectively. Those results show that the photocatalytic activity of the 4.0 mmol/g CdS/rectorite was enhanced significantly comparing with the bare rectorite and the pure CdS. As description in the experimental section, the bulk resistivity of rectorite is about $10^8 \Omega \text{ cm}$, which

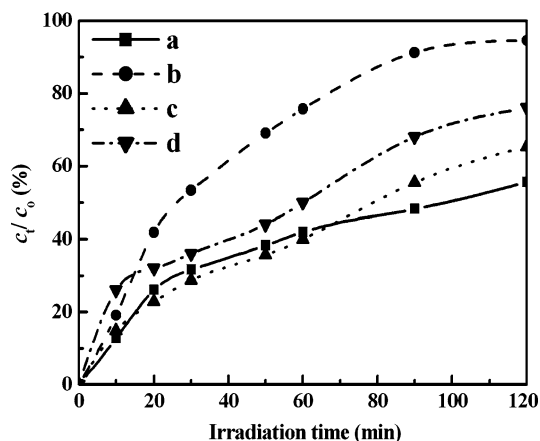


Fig. 9 Photocatalytic activities of the products. **a** Bare rectorite, **b** 4.0 mmol/g CdS/rectorite, **c** physical mixture according to the nominal amount 4.0 mmol/g CdS/rectorite, and **d** pure CdS (11.0 mg) according to 30 mg 4.0 mmol/g CdS/rectorite

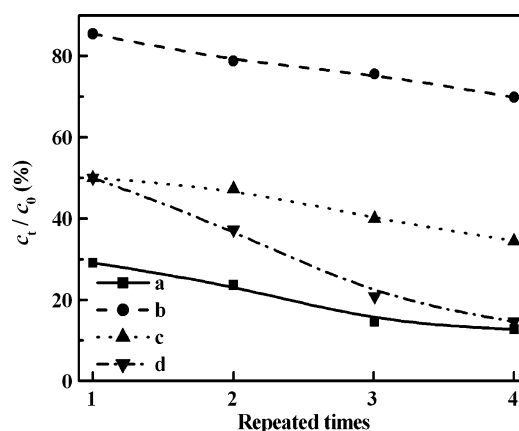


Fig. 10 Photodegradation efficiency changed with the repeated experimental times. **a** Bare rectorite, **b** 4.0 mmol/g CdS/rectorite, **c** physical mixture according to the nominal amount 4.0 mmol/g CdS/rectorite, and **d** pure CdS (11.0 mg) according to 30 mg 4.0 mmol/g CdS/rectorite

intervenes between the insulator and semiconductor. In general, this high resistivity is not beneficial for the electron transfer from CdS to rectorite. Considering the existing of TiO_2 and Fe_2O_3 in the rectorite, and the photocatalytic activity tests are carried out in solution. The photogenerated electrons in guest CdS nano-pillars can quickly transfer through the interlayers into the surfaces of TiO_2 and Fe_2O_3 in the matrix, which is beneficial for retarding the recombination of the photogenerated carriers, and consequently, improving the photoactivity (Shangguan and Yoshida 2001). On the other hand, the relative small CdS particle size is beneficial for the higher photogenerated voltage, more effective electron-hole separation due to the quantum effect. Furthermore, the layer structure is also beneficial for the transfer of the object (RB) and the photo-

degradation products. Therefore, the improved the photoactivity of the CdS/rectorite nanocomposite can be attributed to the cooperation or synergetic action of the inserted CdS, ferric oxide and titania impurities and the specific structure in the rectorite.

The experimental results of photostability for the bare rectorite, the pure CdS, the physical mixture and the 4.0 mmol/g CdS/rectorite are summarized in Fig. 10. Undergoing four times repeated photocatalytic experiments, the photodegradation efficiency of the 4.0 mmol/g CdS/rectorite nanocomposite reduces from 85.4 to 69.8%; but the photodegradation efficiency decreases significantly from 50.0 to 14.6% for the pure CdS. Those results show that the photostability of the nanocomposite is much better than the pure CdS due to the CdS pillars inserted into the interlamellar region of rectorite. The host layer effectively suppress the S^{2-} oxidization, this, consequently, retarded the photocorrosion of the CdS pillars in rectorite (Shangguan and Yoshida 2001).

Conclusion

CdS/rectorite nanocomposites were prepared via a cation-exchanging reaction followed by a sulfurization process. The experimental data indicate that the CdS pillars intercalate into the intergallery spaces of the rectorite and a few of CdS nanoparticles lie in the outer layers. And the CdS nanoparticles in the composites adopt a hexagonal wurtzite structure. The photocatalytic experimental results suggest that the CdS/rectorite nanocomposites show better photocatalytic activities than the bare rectorite and the pure CdS and their physical mixtures according to the nominal amount of CdS/rectorite nanocomposites. Moreover, the photostability of CdS in nanocomposites is also improved compared with the pure one due to the hosts retard the photocorrosion of the CdS. It is interrelated to the cooperation or synergetic action of the CdS, ferric oxide and titania impurities and the specific interlayer structure of the rectorite, which can decrease the recombination of the photogenerated electrons and holes. Those properties are expected to be useful in various applications such as, photodegradation and adsorption of various organic contaminants, photocatalysts for hydrogen production from photosplitting water. In sum, this kind of nanocomposite is potential in energy renewal, energy storage and environmental cleanup as a novel purificatory ecomaterial.

Acknowledgments This work is supported by the Natural Science Fund of China (20573078), National “863” Foundation

(2006AA03Z344), Talented Young Scientist Foundation (2006ABB003) of Hubei Province and the Natural Science Fund(2004ABA083) of Hubei Province, China. Dr. T. Y. Peng is indebted to Dr. J. B. Wang, Center of Electron Microscopy, Wuhan University, who has kindly offered the help in HRTEM observation.

References

- Arora MK, Sahu N, Upadhyay SN, Sinha ASK (1998) Effect of dispersion and distribution on activity of alumina-supported cadmium sulfide photocatalysts for hydrogen production from water. *Ind Eng Chem Res* 37(4):1310–1316
- Arora MK, Sahu N, Upadhyay SN, Sinha ASK (1999) Alumina-supported cadmium sulfide photocatalysts for hydrogen production from water: role of dissolved ammonia in the impregnating solution. *Ind Eng Chem Res* 38(12):4694–4699
- Brindley GW (1956) Allevardite, a swelling double-layer mica mineral. *Am Mineral* 41:91–103
- Dekany I, Turi L, Galbacs G, Fendler JH (1999a) Cadmium ion adsorption controls the growth of CdS nanoparticles on layered montmorillonite and calumite surfaces. *J Colloid Interface Sci* 213(2):584–591
- Dekany I, Turi L, Kiraly Z (1999b) CdS, TiO₂, and Pd nanoparticles growing in the interlamellar space of montmorillonite in binary liquids. *Appl Clay Sci* 15(1–2):221–239
- Fujishiro Y, Uchida S, Sato T (1999) Synthesis and photochemical properties of semiconductor pillared layered compounds. *Int J Inorg Mater* 1(1):67–72
- Grim RE (1968) *Clay mineralogy*. McGraw-Hill Book Co., New York pp 77–92
- Han Z, Zhu H, Bulcock SR, Ringer SP (2005) One-step synthesis and structural features of CdS/montmorillonite nanocomposites. *J Phys Chem B* 109(7):2673–2678
- Hirai T, Okubo H, Komasa I (1999) Size-selective incorporation of CdS nanoparticles into mesoporous silica. *J Phys Chem B* 103(21):4228–4230
- Hong HL, Tie LY, Bian QL, Zhou Y (2005) Study of rectorite from the Zhongxiang (China) deposit, based on SEM and EPMA data. *Dianzi Xianwei Xuebao* 24(2):124–128
- HuBei Province Gelology and Mineral Office (1989) *Rectorite*, HuBei Science and Technology Press, Wuhan, China, pp 38–61
- Katsikas L, Eychmueller A, Giersig M, Weller H (1990) Discrete excitonic transitions in quantum-sized cadmium sulfide particles. *Chem Phys Lett* 172(3–4):201–204
- Kooli F, Bovey J, Jones W (1997) Dependence of the properties of titanium-pillared clays on the host matrix: a comparison of montmorillonite, saponite and rectorite pillared materials. *J Mater Chem* 7(1):153–158
- Lu Q, Tang Z, Lei X, Liu H, Liu Y (2001) Research of Ti-Pillared rectorite mineralogica sinica materials (In Chinese). *Acta Mineralogica Sin* 21(1):27
- Malla P, Yamanaka S, Komarneni S (1989) Unusual water vapor adsorption behavior of montmorillonite pillared with ceramic oxides. *Solid State Ionics* 32–33(PtI):354–362
- Minoura H, Tsuiji M (1978) Anodic reactions of several reducing agents on illuminated cadmium sulfide electrode. *Electrochim Acta* 23(12):1377–1382
- Occelli ML (1991) Scientific basis for the preparation of heterogeneous catalysts. In: Fifth international symposium, Elsevier, Amsterdam, pp 287–289
- Occelli ML, Gould SAC (2001) Examination of coked surfaces of pillared rectorite catalysts with the atomic force microscope. *J Catal* 198(1):41–46

- Occelli ML, Auroux A, Ray GJ (2000a) Physicochemical characterization of a Texas montmorillonite pillared with polyoxocations of aluminum. II. NMR and microcalorimetry results. *Microporous Mesoporous Mater* 39(1–2):43–56
- Occelli ML, Bertrand JA, Gould SAC, Dominguez JM (2000b) Physicochemical characterization of a Texas montmorillonite pillared with polyoxocations of aluminum. Part I. The microporous structure. *Microporous Mesoporous Mater* 34(2):195–206
- Occelli ML, Dominguez JM, Eckert H (1993) Vanadium effects on pillared rectorite catalysts. *J Catal* 141(2):510–523
- Ohtsuka K (1997) Preparation and properties of two-dimensional microporous pillared interlayered solids. *Chem Mater* 9(10):2039–2050
- Pichowicz M, Mokaya R (2004) Stability of pillared clays: effect of compaction on the physicochemical properties of Al-pillared clays. *Chem Mater* 16(2):263–269
- Sapra S, Nanda J, Sarma DD, Abed El-Al F, Hodes G (2001) Blue emission from cysteine ester passivated cadmium sulfide nanoclusters. *Chem Commun* 21:2188–2189
- Sato T, Masaki K, Sato K, Fujishiro Y, Okuwaki A (1996a) Photocatalytic properties of layered hydrous titanium oxide/CdS-ZnS nanocomposites incorporating CdS-ZnS into the interlayer. *J Chem Technol Biotechnol* 67(4):339–344
- Sato T, Sato K, Fujishiro Y, Yoshioka T, Okuwaki A (1996b) Photochemical reduction of nitrate to ammonia using layered hydrous titanate/cadmium sulfide nanocomposites. *J Chem Technol Biotechnol* 67(4):345–349
- Schwerzel RE, Spahr KB, Kurmer JP, Wood VE, Jenkins JA (1998) Nanocomposite photonic polymers. 1. Third-order nonlinear optical properties of capped cadmium sulfide nanocrystals in an ordered polydiacetylene host. *J Phys Chem A* 102(28):5622–5626
- Shangguan WF, Yoshida A (2001) Synthesis and photocatalytic properties of CdS-intercalated metal oxides. *Solar Energy Mater Solar Cells* 69(2):189–194
- Stramel RD, Nakamura T, Thomas JK (1986) Cadmium sulfide on synthetic clay. *Chem Phys Lett* 130(5):423–425
- Thomas SM, Occelli ML (2000) Effects of synthesis conditions on the thermal stability of a Texas montmorillonite expanded with $[Al_{13}O_4(OH)_{24}(H_2O)_{12}]^{7+}$ cations. *Clays Clay Minerals* 48(2):304–308
- Wang S, Choi DG, Yang SM (2002) Incorporation of CdS nanoparticles inside ordered mesoporous silica SBA-15 via ion exchange. *Adv Mater* 14(18):1311–1314
- Xie Y, Zhang G, Zhu C, Yu J (2004) Synthesis of TiO_2 /rectorite and study on its photocatalytic activity (In Chinese). *Ind Safety Environ Prot* 30(7):28–30
- Yamanaka S, Malla PB, Komarneni S (1990) Water adsorption properties of alumina pillared clay. *J Colloid Interface Sci* 134(1):51–58
- Zhang Z, Dai S, Fan X, Blom DA, Pennycook SJ, Wei Y (2001) Controlled synthesis of CdS nanoparticles inside ordered mesoporous silica using ion-exchange reaction. *J Phys Chem B* 105(29):6755–6758
- Zhang G, Yang X, Liu Y, Jia Y, Yu G, Ouyang S (2004) Copper(II) adsorption on Ca-rectorite, and effect of static magnetic field on the adsorption. *J Colloid Interface Sci* 278(2):265–269
- Zhang G, Liu Y, Xie Y, Yang X, Hu B, Ouyang S, Liu H, Wang HY (2005) Zinc adsorption on Na-rectorite and effect of static magnetic field on the adsorption. *Appl Clay Sci* 29(1):15–21